AN IMPROVED NONLINEAR CONTROL STRATEGY FOR INDUCTION MOTOR DRIVE

Guang Feng *Yanfei Liu*

Department of Electrical and Computer Engineering, Queens University
Kingston, Ontario, K7L 3N6
Email: guang.feng@ece.queensu.ca, yanfei.liu@ece.queensu.ca

ABSTRACT

In this paper, a new configuration called Auto Disturbance Rejection Controller (ADRC) is used in the induction motor speed control. The key part of ADRC is extended state observer (ESO). By using ESO, ADRC can estimate accurately the derivative signals and accurate decoupling of induction motor is achieved too. In addition, the external disturbances and parameter variations could also be estimated and compensated by ADRC, so that the closed loop motor drive system under ADRC control does not depend on the accurate mathematical model of induction motors. Therefore, the robustness and adaptability of the control system is improved too. The simulation and experiment results show that the controller operates quite robustly under modeling uncertainty and external disturbance, and it can provide good dynamic performance such as small overshoot and fast transient time in the speed control.

1. INTRODUCTION

High dynamic performance of induction motors is needed in a lot of industrial applications. At present, vector control appears much more attractive because of the capability of torque/flux decoupling which gives high dynamic response and accurate motion control. Unfortunately in real-time implementation, the torque and flux will not be completely decoupled due to significant plant uncertainties such as external disturbances, unpredictable parameter variations and unmodeled plant nonlinear dynamics [1]. This deteriorates the dynamic performance of induction motor significantly. In addition, the performance of this control system depends on the accurate mathematical model of induction motors [2]. Conventional method in vector control is to use PID controllers to regulate the static and dynamic performance of control system. In PID controller, the derivatives of the signals are required in order to achieve control objectives, such as reduced response time and reduced overshoot during transient conditions. Unfortunately, the derivatives of signals are difficult to retrieve because of noise. Furthermore, the performance of PID controller often deteriorates at different operating conditions. In recent years, adaptive methods and predict PID controllers are proposed to improve the robustness and dynamic performance of control system [3-7]; however they are very complicated and have much computational intensity in the real-time implementation.

Based on the concept of generalized derivative, in this paper, a new configuration called Auto-Disturbance Rejection Controller (ADRC) is used in the induction motor speed control. The core of ADRC is the extended state observer. By using the extended state observer, ADRC can estimate accurately the derivative signals and the coupling part of d-axis and q-axis. Accurate decoupling of induction motor can be achieved. In addition, the external disturbances and parameter variations could also be estimated and compensated by ADRC, so that the accurate model of induction model is not required. That means the design of ADRC is independent of the controlled system model, and this controller can achieve good adaptability and robustness as well. The simulation and experiment results show that ADRC can provide good dynamic performance under large variations of drive system parameters and load conditions.

2. CONTROL STRATEGY

The structure of nonlinear auto-disturbance rejection controller is shown in Fig.1. ADRC is composed of three parts: tracking-differentiator (TD), extended state observer

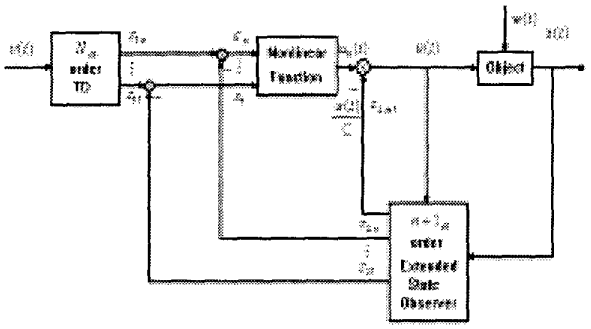

Fig. 1. The Block Diagram of ADRC

(ESO) and nonlinear state error feedback control law (NLSEF) [8]. The key part of ADRC is (N+1)th order ESO, which uses nonlinear state feedback to realize the linearization of uncertain nonlinear systems. Unlike full order (Nth order) state observer, ESO utilizes (N+1)th order (full order plus 1) state observation to achieve feedback linearization. In ESO, lower order derivative is obtained by integrating the higher order derivatives. No differential operation is needed. Therefore, the differential signal is obtained without noises. Furthermore, the signal of (N+1)th state variable reveals the information about disturbances and plant uncertainties in the control system. When the nonlinear functions and their related parameters of ESO are properly selected, the state variables $z_i(t)$ $i = 1, \cdots, n$ of ESO will converge to the observed state variables $x(t)$ and its derivatives. At the same time, the external and internal disturbances can also be observed.

The observer's architecture is not determined by the actual expression of system under control, but only affected by its variation range. Therefore, this observer has very good robustness and adaptability.

Tracking-Differentiator (Nth order TD in the Fig.1) is a dynamic system which can arrange the transition process according to the input reference signal and the system under control. Comparing the difference between the output of tracking-differentiator and extended state observer, nonlinear state error feedback control law $u(t)$ is used to drive the state trajectory to the desired reference signal. With the help of modeling uncertainty and disturbance compensation, this control system will have desired behaviors such as tracking, regulation, stability, etc.

3. ADRC FOR INDUCTION MOTOR

Based on the reference-frame theory and the rotor flux orientation, the state space model of a squirrel case induction motor in a synchronous d-q reference frame can be described by fourth order nonlinear differential equation:

$$\begin{cases} \dot{i}_{d1} = -k_1 i_{d1} + k_2 \psi_{d2} + i_{q1}\omega_1 + \dfrac{1}{\sigma} u_{d1} \\ \dot{\psi}_{d2} = \dfrac{L_m}{T_r} i_{d1} - \dfrac{1}{T_r}\psi_{d2} \\ \dot{\omega}_r = k_3 \psi_{d2} i_{q1} - T_L n_p / J \\ \dot{i}_{q1} = -k_1 i_{q1} - \dfrac{L_m}{\sigma L_r}\psi_{d2}\omega_r - i_{d1}\omega_1 + \dfrac{1}{\sigma} u_{q1} \end{cases} \quad (1)$$

where

$T_r = \frac{L_r}{R_r}$ $\quad \sigma = L_s - \frac{L_m^2}{L_r}$

$k_1 = \frac{R_s L_r^2 + R_r L_m^2}{\sigma L_r^2}$ $\quad k_2 = \frac{R_r L_m}{\sigma L_r^2}$ $\quad k_3 = \frac{n_p^2 L_m}{J L_r}$

u_{d1}, u_{q1}	d-axis(q-axis)stator volage
i_{d1}, i_{q1}	d-axis(q-axis)statorcurrent
ψ_{d2}, ψ_{q2}	d-axis(q-axis)rotorflux
ω_1	rotatingspeedof thecoordinate
ω_r	rotorangularspeed
T_L	loadtorque
R_s, R_r	stator and rotor resistances
L_s, L_r, L_m	stator, rotor and mutual inductances
J	rotor inertia
n_p	pole pairs

The above equations show that
(1) The system is nonlinear due to the coupling parts between state variables.
(2) The variation of motor parameters will deteriorate the performance of the drive system.

In this paper, we assume ω_r, ψ_{d2}, i_{d1}, i_{q1} and their derivatives exist and are continuous. As it is shown in equation (1), the rotor flux is mainly controlled by first and second item of equation (1); the speed is affected mainly by the third and fourth item of equation (1).
From equation (1), the 2nd derivative of flux is obtained as follows:

$$\ddot{\psi}_{d2} = -\frac{1}{T_r}\dot{\psi}_{d2} + \frac{L_m}{T_r} k_2 \psi_{d2} + \frac{L_m}{T_r}(-k_1 i_{d1} + i_{q1}\omega_1) + \frac{L_m}{T_r \sigma} u_{d1} \quad (2)$$

If the coupling part of equation (2)-- $\frac{L_m}{T_r}(-k_1 i_{d1} + i_{q1}\omega_1)$ is regarded as the modeling disturbance of system, it can be rewritten as:

$$\ddot{\psi}_{d2} = -\frac{1}{T_r}\dot{\psi}_{d2} + \frac{L_m}{T_r} k_2 \psi_{d2} + w_{11}(t) + \frac{L_m}{T_r \sigma} u_{d1} \quad (3)$$

Where $w_{11}(t) = \frac{L_m}{T_r}(-k_1 i_{d1} + i_{q1}\omega_1)$

Similarly, the coupling part in the derivatives of ω_r and i_{q1} can be treated as modeling disturbance as

following:

$$\begin{cases} \dot{\omega}_r = k_3 \psi_{d2} i_{q1} + w_{21}(t) \\ \dot{i}_{q1} = -k_1 i_{q1} + w_{31}(t) + \dfrac{1}{\sigma} u_{q1} \end{cases} \tag{4}$$

Where

$$w_{21}(t) = -T_L n_p / J \square w_{31}(t) = -\frac{L_m}{\sigma L_2} \psi_{d2} \omega_r - i_{d1} \omega_1$$

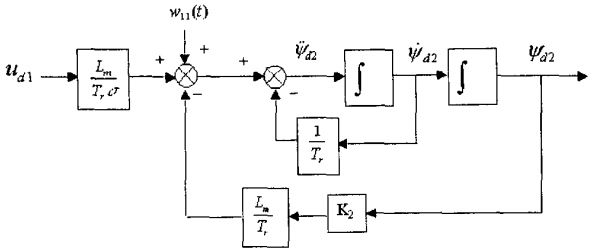

(a) Flux Subsystem

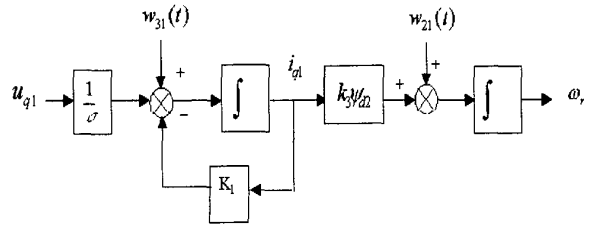

(b) Speed Subsystem

Fig. 2. The Equivalent Dynamic Mathematical Model of Induction Motor

If we select the control voltage reference as:

$$u_{d0} = \frac{w_{11}(t)}{L_m / (T_r \sigma)} + u_{d1} \tag{5}$$

$$I_{q0} = i_{q1} + w_{21}(t) / (k_2 \psi_{d2}) \tag{6}$$

$$u_{q0} = w_{31}(t) \cdot \sigma + u_{q1} \tag{7}$$

Then, the coupling between the torque-producing current i_{q1} and the rotor flux ψ_{d2} can be completely eliminated. The closed loop system can be simplified as:

$$\ddot{\psi}_{d2} = -\frac{1}{T_r}\dot{\psi}_{d2} + \frac{L_m}{T_r} k_2 \psi_{d2} + \frac{L_m}{T_r \sigma} u_{d0} \tag{8}$$

$$\dot{\omega}_r = k_3 \psi_{d2} I_{q0}$$

$$\dot{i}_{q1} = -k_1 i_{q1} + \frac{1}{\sigma} u_{q0}$$

The model of induction model can be decoupled into two linear subsystems: flux subsystem and speed subsystem (shown in Fig.2). It can be observed from Fig. 2 that the precise decoupling of flux and speed control and exact linearization can be achieved if the ESO can realize

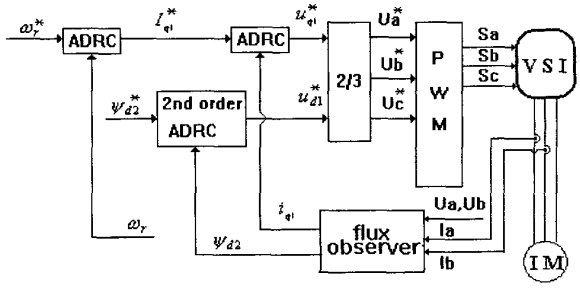

Fig. 3. The Control System of Induction Motor

the state feedback and model compensation. So, it is convenient to use ADRC to give control signal u_{d1} and I_{q0}, u_{q1} [9].

Considering the external disturbance and parameter variation (we use the rotor resistant change and load disturbance as a example), the equation (3), (4) can be rewritten as follows,

$$\ddot{\psi}_{d2} = -\frac{1}{T_r}\dot{\psi}_{d2} + \frac{L_m}{T_r} k_2 \psi_{d2} + w_{11}(t) + \frac{L_m}{T_r \sigma} u_{d1} + w_{12}(t) \tag{9}$$

$$w_{12}(t) = (\frac{1}{T_r} - \frac{1}{T_r'})\dot{\psi}_{d2} + (\frac{L_m}{T_r'} k_2' - \frac{L_m}{T_r} k_2)\psi_{d2} + (\frac{L_m}{T_r' \sigma'} - \frac{L_m}{T_r \sigma}) u_{d1}$$

$$\begin{cases} \dot{\omega}_r = k_3 \psi_{d2} i_{q1} + w_{21}(t) + w_{22}(t) \\ \dot{i}_{q1} = -k_1 i_{q1} + w_{31}(t) + \dfrac{1}{\sigma} u_{q1} + w_{32}(t) \end{cases} \tag{10}$$

where

$$w_{22}(t) = \Delta k_3 \psi_{d2} i_{q1} + \Delta T_L n_p / J$$

$$w_{32}(t) = \Delta k_1 i_{q1} + \Delta(\frac{1}{\sigma}) u_{q1}$$

In the above model, the external load change and internal parameter variation are all treated as disturbances imposed on the control system. As the variation range of load and parameter change is finite, we can estimate and compensate the model parameter variation and external disturbance by properly selecting the functions and related parameters of ESO and ADRC. The above analysis has shown that the closed loop motor drive system under ADRC control does not depend on the accurate mathematical model of induction motors. Therefore, the robustness and adaptability of the control system is significantly improved.

Fig.3 shows the proposed ADRC for induction motor. In order to achieve the rotor angular speed and the rotor flux regulation, the controller includes two distinct control loops: the flux loop which employs one 2nd ADRC to regulate the rotor flux; the speed loop, which employs two 1st order ADRC to control the rotor speed ω_r and q-axis stator current i_{q1}.

4. RESULTS

The proposed ADRC and its performance are now verified by simulation and experiments. The parameters of a 2.2 kW induction motor are as follows:

Rs=2.92 Ω Rr=1.92 Ω Ls=0.371 H
Lr=0.371 H Lm=0.358 H Polepairs=2
$J = 0.1\,\mathrm{kg} \cdot \mathrm{m}^2$ Rated Speed = 1430 *rpm*

4.1. Simulation Results

All simulations are done with a load torque change applied to the induction motor. To see the influence of the proposed controller, the performances of ADRC and classic PID controller are compared. In order to limit the noises that exist in the detected signals, the coefficient of differentiator in PID controller is small.

Fig. 4 shows the actual and estimated rotor angular speed ω_r of start up. At t=1.1s, load torque $T_L = 15\mathrm{N}\cdot\mathrm{m}$ is added to the induction motor. Fig. 5 shows the derivative of rotor angular speed including the actual value and the value estimated by ESO. The simulation results demonstrate that the extended state observer can track the state variables of the induction motor and their derivatives successfully.

Fig. 6 shows dynamic responses of ADRC and PID controller with step disturbance load ($T_L = 15N \cdot m$). For ADRC, the speed response under rated speed shows no overshoot and it settles down quickly to a steady state without steady state error.

In order to show ADRC wide operation range, the parameters of the ADRC and PID controller have been optimized at rated speed (1430 rpm). Then, the same controllers are applied to regulate the induction motor at low speed (10 r/min) without changing their parameters. The performances of PID controller deteriorate, while ADRC can maintain its excellent performance (Shown in Fig.7). It shows ADRC could maintain its good dynamics and robustness to load disturbance in various operating conditions.

4.2. Experiment Results

Fig 8, 9 show the speed curves of the induction motor with load torque $T_L = 6N \cdot m$ while setting rotor speed is changed. From these figures, we can see that the ADRC can maintain better dynamic performance and adaptability than PID controller over wide speed range.

In order to testify the robustness of ADRC under parameter variation, we reset the value of given rotor resistance in the model of induction motor to be approximately 50% lower (from 1.92Ω→1.0Ω) or 25% higher (from 1.92Ω→2.5Ω) than that of the actual rotor resistance separately. After that, we operate the ADRC and PID controller in the same condition. From Fig 10, we can see that the ADRC can achieve no overshoot and small transient time during start up while dynamic performance of PID controller has deteriorated. Fig.11 to Fig.14 show the experimental tests of ADRC and PID controller under given rotor resistance change. We can see that the dynamic performance of PID controller deteriorate significantly while ADRC maintains good speed regulation under parameter changes. From these figures, it can be noted that ADRC can achieve good robustness and adaptability to external and internal disturbances.

5. CONCLUSION

This paper presented a new robust nonlinear controller for induction motor. ADRC is used to implement the state estimation and achieve robustness against motor parameter's change and load variation. The major advantage of the proposed method is that the closed loop characteristics of the motor drive system do not depend on the exact mathematical model of induction motor. No derivative calculation is needed either. From simulation and experiment results, it is observed that proposed ADRC control system is robust against the modeling uncertainty and the external disturbance. These results open new perspectives on utilization of nonlinear controllers on field orientation, and promote a new stream of studies on developing different structures of this class of controllers.

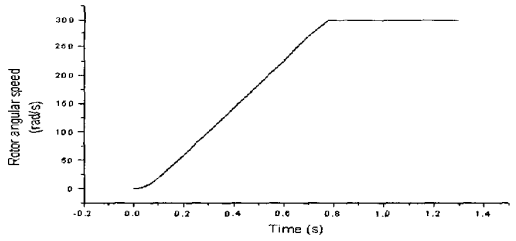

Fig. 4 actual (solid line) and estimated (dashed line) rotor angular speed ω_r

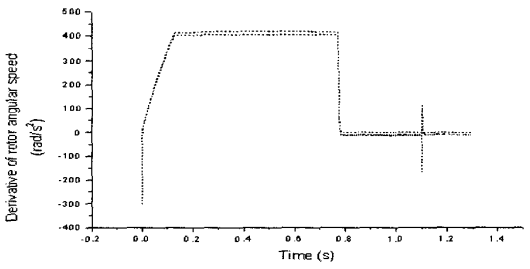

Fig.5 actual (solid line) and estimated (dashed line) rotor angular speed derivative

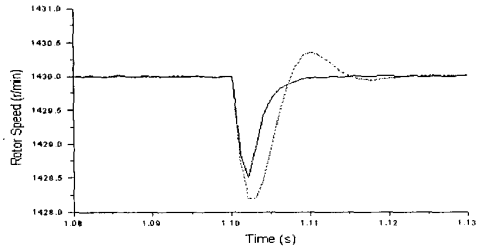

Fig. 6 dynamic speed responses of ADRC (solid line) and PID controller (dashed line) due to load torque change (from 0 – 15 N · m) at rated speed

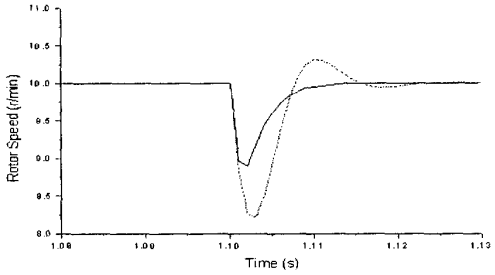

Fig. 7 dynamic responses of speed regulation at low speed (10 r/min) --- Using ADRC (solid line); Using PID controller (dashed line)

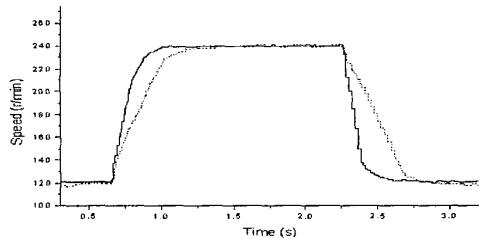

Fig. 8 dynamic speed responses of induction motor (changed from 120 to 240r/min)--- ADRC (solid line); PID controller (dashed line)

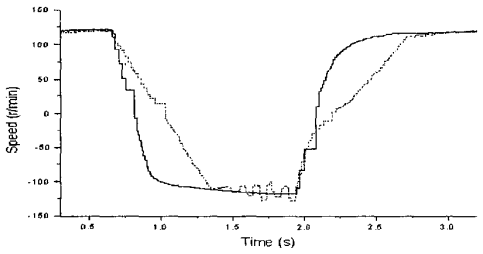

Fig. 9 dynamic speed responses of induction motor (changed from 120 to –120r/min) --- ADRC (solid line); PID controller (dashed line)

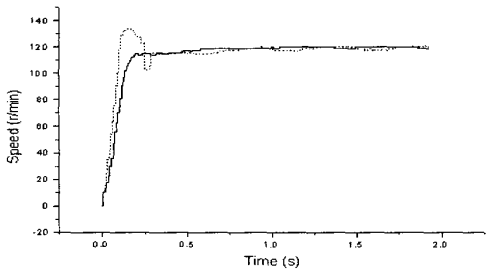

Fig. 10 dynamic speed responses of induction motor when starting up under rotor resistant change (from 1.92Ω→1.0Ω□--- ADRC (solid line); PID controller (dashed line)

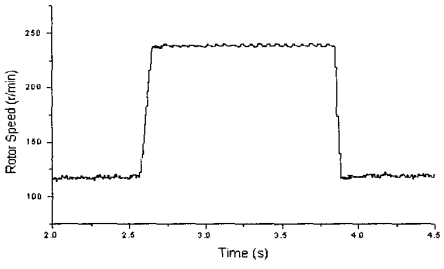

(a) ADRC

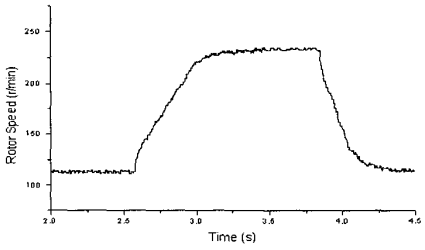

(b) PID Controller

Fig. 11 dynamic speed responses of induction from 120 to 240r/min under rotor resistant change (from 1.92Ω→1.0Ω)

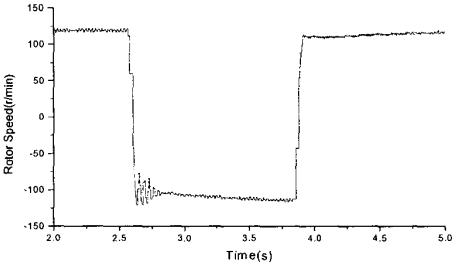

(a) ADRC

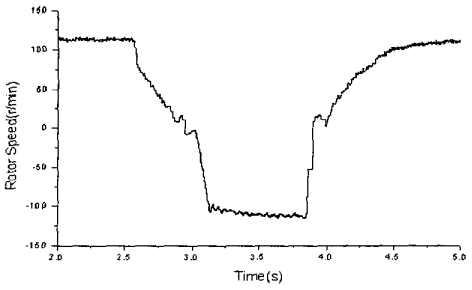

(b) PID Controller

Fig. 12 dynamic speed responses of induction from 120 to −120r/min under rotor resistant change (from 1.92Ω→1.0Ω)

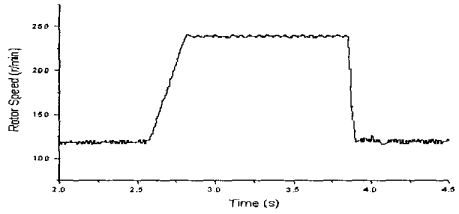

(a) ADRC

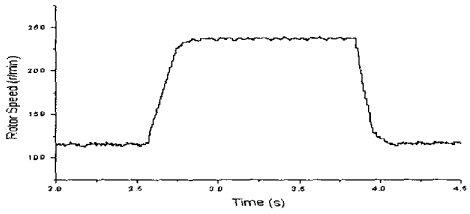

(b) PID Controller

Fig. 13 dynamic speed responses of induction from 120 to 240r/min under rotor resistant change (from 1.92Ω→2.5Ω)

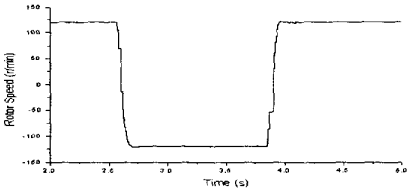

(a) ADRC

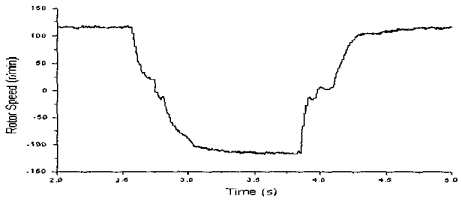

(b) PID Controller

Fig. 14 dynamic speed responses of induction from 120 to −120r/min under rotor resistant change (from 1.92Ω→2.5Ω)

REFERENCES

[1] Special Issue on Power Electronics and Motion Control, *Proc. IEEE*, vol. 82, no. 8, Aug. 1994.

[2] R.S.Cabrera and J.Morales, "Some results about the control and observation of induction motors", in *Proceedings of the 1995 IEEE American Control Conference*, 95CH35736, pp. 1633-1637.

[3] Y. Ping, D. Vrancic, and R. Hanus, "Anti-windup, bumpless, and conditioned transfer techniques for PID controllers," *IEEE Trans. Contr. Syst. Technol.*, vol. 16, pp. 48-57, July 1996.

[4] K. J. Astrom and T. Hagglund, Automatic Tunning of PID Controllers, *Instrument Society of America, Research Triangle Park, NC*, pp.3-28, 1998.

[5] N. J. Krikelis and S. K. Barkas, "Design of tracking systems subject to actuator saturation and integral wind-up", *Int. J. Control*, vol. 39, no. 4, pp. 667-682, 1984.

[6] Chen Jie,Li Yongdong, "Virtual Vectors Based Predictive Control of Torque and Flux of Induction Motor and Speed Sensorless Drives", *IEEE IAS 99*, pp 2606-2613.

[7] C. Cecati, G. Guidi, et.al, "An adaptive non-linear control algorithm for induction motor", in *Proceedings of the 1996 IEEE IECON*, pp.326-331, vol.1.

[8] J. Han, "Auto-disturbances-rejection Controller and It's Applications", *Trans. Control and Decision*, China, vol.13, No.1, pp19-23, 1998.

[9] Guang Feng, Lipei Huang and Dongqi Zhu, "A Nonlinear Auto-Disturbance Rejection Controller for Induction Motor", *IEEE IECON'98*, vol.3, pp1509-1514.